Spin-polarized transport through a single-level quantum dot in the Kondo regime

2006 J. Phys.: Condens. Matter 18 2291

(http://iopscience.iop.org/0953-8984/18/7/016)

INSTITUTE OF PHYSICS PUBLISHING JOURNAL OF PHYSICS: CONDENSED MATTER

J. Phys.: Condens. Matter **18** (2006) 2291–2304 doi:10.1088/0953-8984/18/7/016

Spin-polarized transport through a single-level quantum dot in the Kondo regime

R Świrkowicz[1], **M Wilczyński**[1] **and J Barnaś**[2,3]

[1] Faculty of Physics, Warsaw University of Technology, ulica Koszykowa 75, 00-662 Warszawa, Poland
[2] Department of Physics, Adam Mickiewicz University, ulica Umultowska 85, 61-614 Poznań, Poland
[3] Institute of Molecular Physics, Polish Academy of Sciences, ulica Smoluchowskiego 17, 60-179 Poznań, Poland

E-mail: barnas@main.amu.edu.pl

Received 20 August 2005, in final form 4 January 2006
Published 3 February 2006
Online at stacks.iop.org/JPhysCM/18/2291

Abstract

Nonequilibrium electronic transport through a quantum dot coupled to ferromagnetic leads (electrodes) is studied theoretically by the nonequilibrium Green function technique. The system is described by the Anderson model with arbitrary correlation parameter U. Exchange interaction between the dot and ferromagnetic electrodes is taken into account *via* an effective molecular field. The following situations are analysed numerically: (i) the dot is symmetrically coupled to two ferromagnetic leads, (ii) one of the two ferromagnetic leads is half-metallic with almost total spin polarization of electron states at the Fermi level, and (iii) one of the two electrodes is nonmagnetic whereas the other one is ferromagnetic. Generally, the Kondo peak in the density of states (DOS) becomes spin-split when the total exchange field acting on the dot is nonzero. The spin-splitting of the Kondo peak in DOS leads to splitting and suppression of the corresponding zero-bias anomaly in the differential conductance.

1. Introduction

The Kondo phenomenon in electronic transport through artificial quantum dots (QDs) or single molecules attached to nonmagnetic leads was predicted theoretically more than a decade ago [1]. Owing to recent progress in nanotechnology, the phenomenon has been also observed experimentally [2, 3]. Several theoretical techniques have been developed to describe this effect [4–11]. The description is usually simpler in the linear response regime, where equilibrium methods can be applied, but it becomes more complex when the system is driven out of equilibrium by an external bias voltage [7, 11–15]. One of the methods used to describe the nonequilibrium Kondo effect is the nonequilibrium Green function technique [5, 16, 17]. To

calculate the density of states (DOS) and electric current one then needs the retarded/advanced as well as the lesser (correlation) Green functions. These can be derived within some approximation schemes.

It has been shown recently that the Kondo effect can also occur when replacing nonmagnetic leads by ferromagnetic ones [18–22], but ferromagnetism of the electrodes generally suppresses the effect—either partially or totally [19, 22]. However, in some peculiar situations the effect remains almost unchanged. Suppression of the Kondo anomaly is a consequence of an effective exchange field due to coupling between the dot and ferromagnetic electrodes. The exchange field gives rise to spin-splitting of the equilibrium Kondo peak in the DOS, and the two components of the split peak move away from the Fermi level, which leads to suppression of the Kondo anomaly in the electrical conductance—similarly as an external magnetic field suppresses the effect in nonmagnetic systems. Such a suppression was studied recently by the Green function technique in the limit of the infinite correlation parameter U [19], and was also confirmed by numerical renormalization group calculations [23, 24]. However, only QDs symmetrically coupled to two magnetic leads have been studied up to now. The Kondo anomaly survives then in the antiparallel magnetic configuration and is significantly suppressed in the parallel one. Recent experimental observations on C_{60} molecules attached to ferromagnetic (Ni) electrodes support these general theoretical predictions [25].

Some features of the nonequilibrium Kondo phenomenon in QDs coupled to ferromagnetic leads have not been addressed yet. Therefore, in this paper we consider a more general situation. First of all, we consider the case when the two ferromagnetic electrodes are generally different. In other words, the dot is (spin-)asymmetrically coupled to the ferromagnetic leads. This leads to qualitatively new results. Second, we consider the case of arbitrary U instead of the limiting situation of infinite U studied in [19]. Third, we introduce an effective exchange field to describe the dot level renormalization.

We analyse in detail three different situations. In the first case the dot is coupled to two ferromagnetic leads, and the coupling is fully symmetric in the parallel magnetic configuration. We show that the equilibrium Kondo peak in the DOS is then spin-split in the parallel configuration, whereas no splitting appears in the antiparallel one. The splitting, however, is significantly reduced for small values of the correlation parameter U. The corresponding zero-bias anomaly in the conductance becomes split in the parallel configuration as well [19]. The second situation studied in this paper is the one with asymmetric coupling to two ferromagnetic leads. As a particular case we consider the situation when one of the ferromagnetic electrodes is half-metallic, with almost total spin polarization of electron states at the Fermi level. Such structures have been shown recently to have transport characteristics with typical diode-like behaviour [26, 27]. Finally, we also analyse the case when one of the electrodes is nonmagnetic whereas the second one is ferromagnetic, and show that one ferromagnetic electrode is sufficient to generate spin-splitting of the Kondo anomaly.

The paper is organized as follows. The model and method are briefly described in sections 2 and 3, respectively. Numerical results for the three different situations mentioned above are presented and discussed in section 4. A summary and general conclusions are given in section 5.

2. Model

We consider a single-level QD coupled to ferromagnetic metallic leads (electrodes) by tunnelling barriers. We restrict our considerations to collinear (parallel and antiparallel) magnetic configurations and assume that the axis z (spin quantization axis) points in the direction of the net spin of the left electrode (opposite to the corresponding magnetic moment).

Antiparallel alignment is obtained by reversing magnetic moment of the right electrode. The whole system is then described by a Hamiltonian of the general form

$$H = H_{\mathrm{L}} + H_{\mathrm{R}} + H_{\mathrm{D}} + H_{\mathrm{T}}. \tag{1}$$

The terms H_β describe here the left ($\beta = \mathrm{L}$) and right ($\beta = \mathrm{R}$) electrodes in the noninteracting quasiparticle approximation, $H_\beta = \sum_{k\sigma} \varepsilon_{k\beta\sigma} c^\dagger_{k\beta\sigma} c_{k\beta\sigma}$, where $\varepsilon_{k\beta\sigma}$ is the single-electron energy in the electrode β for the wavenumber k and spin σ ($\sigma = \uparrow, \downarrow$), whereas $c^\dagger_{k\beta\sigma}$ and $c_{k\beta\sigma}$ are the corresponding creation and annihilation operators. The single-particle energy $\varepsilon_{k\beta\sigma}$ includes the electrostatic energy due to applied voltage, $\varepsilon_{k\beta\sigma} = \varepsilon^0_{k\beta\sigma} + eU^\beta_e = \varepsilon^0_{k\beta\sigma} + \mu_\beta$, where $\varepsilon^0_{k\beta\sigma}$ is the corresponding energy in the unbiased system, U^β_e is the electrostatic potential of the βth electrode, e stands for the electron charge ($e < 0$), and μ_β is the chemical potential of the βth electrode (the energy is measured from the Fermi level of unbiased system). The electron spin projection on the global quantization axis is denoted as $\uparrow$ for $s_z = 1/2$ and $\downarrow$ and for $s_z = -1/2$. On the other hand, the spin projection on the local quantization axis (local spin polarization in the ferromagnetic material) will be denoted as $+$ for spin-majority and $-$ for spin-minority electrons, respectively. When local and global quantization axes coincide, then $\uparrow$ is equivalent to $+$ and $\downarrow$ is equivalent to $-$. (Note that the local quantization axis in the ferromagnet is opposite to the local magnetization.)

The term H_{D} in equation (1) describes the quantum dot and takes the form

$$H_{\mathrm{D}} = \sum_\sigma \epsilon_\sigma d^\dagger_\sigma d_\sigma + U d^\dagger_\uparrow d_\uparrow d^\dagger_\downarrow d_\downarrow, \tag{2}$$

where ϵ_σ denotes the energy of the dot level (spin-dependent in a general case), U denotes the electron correlation parameter, whereas $d^\dagger_\sigma$ and d_σ are the creation and annihilation operators for electrons on the dot. The level energy ϵ_σ includes the electrostatic energy due to applied voltage, $\epsilon_\sigma = \epsilon_{0\sigma} + eU^d_e$, where U^d_e is the electrostatic potential of the dot, and $\epsilon_{0\sigma}$ is the level energy at zero bias.

The electrostatic potential U^d_e of the dot will be determined fully self-consistently from the following capacitance model [28, 29]:

$$e\left(\sum_\sigma n_\sigma - \sum_\sigma n_{0\sigma}\right) = C_{\mathrm{L}}(U^d_e - U^{\mathrm{L}}_e) + C_{\mathrm{R}}(U^d_e - U^{\mathrm{R}}_e), \tag{3}$$

where n_σ and $n_{0\sigma}$ are the dot occupation numbers $\langle d^+_\sigma d_\sigma \rangle$ calculated for a given bias and for zero bias, respectively, whereas C_{L} and C_{R} denote the capacitances of the left and right tunnel junctions. Self-consistent determination of the dot electrostatic potential makes the description gauge invariant. This is particularly important for strongly asymmetric systems.

The last term, H_{T}, in equation (1) describes tunnelling processes between the dot and electrodes and is of the form

$$H_{\mathrm{T}} = \sum_{k\beta\sigma} V^*_{k\beta\sigma} c^\dagger_{k\beta\sigma} d_\sigma + \mathrm{h.c.}, \tag{4}$$

where $V_{k\beta\sigma}$ are the components of the tunnelling matrix, and H.c. stands for the Hermitian conjugate term. The Hamiltonian (4) includes only spin-conserving tunnelling processes.

3. Theoretical formulation

The electric current flowing from the βth lead to the quantum dot in a nonequilibrium situation is determined by the retarded (advanced) $G^{r(a)}_\sigma$ and correlation (lesser) $G^<_\sigma$ Green functions of

the dot (calculated in the presence of coupling to the electrodes), and is given by the formula [30]

$$I_\sigma^\beta = \frac{ie}{\hbar}\int \frac{dE}{2\pi}\Gamma_\sigma^\beta(E)\{G_\sigma^<(E) + f_\beta(E)[G_\sigma^r(E) - G_\sigma^a(E)]\}, \tag{5}$$

where $f_\beta(E)$ is the Fermi distribution function for the βth electrode. The retarded (advanced) Green functions can be calculated from the corresponding equation of motion. The key difficulty is with calculating the lesser Green function $G_\sigma^<(E)$.

In the following we assume constant (independent of energy) coupling parameters, $\Gamma_\sigma^\beta(E) = 2\pi\sum_k V_{k\beta\sigma}V_{k\beta\sigma}^*\delta(E-\varepsilon_{k\beta\sigma}) = \Gamma_\sigma^\beta$. As pointed out in [33, 34], it is then sufficient to determine $\int(dE/2\pi)\,G_\sigma^<(E)$, while knowledge of the exact form of $G_\sigma^<(E)$ is not necessary. The current conservation condition allows us then to express the above integral by an integral including retarded and advanced Green functions only, which in turn allows us to rewrite the current formula in the commonly used form,

$$I_\sigma = \frac{ie}{\hbar}\int \frac{dE}{2\pi}\frac{\Gamma_\sigma^L\Gamma_\sigma^R}{\Gamma_\sigma^L+\Gamma_\sigma^R}[G_\sigma^r(E) - G_\sigma^a(E)][f_L(E) - f_R(E)]. \tag{6}$$

Similarly, the occupation numbers, $n_\sigma = \langle d_\sigma^\dagger d_\sigma\rangle$, are then given by the formula

$$n_\sigma = -i\int \frac{dE}{2\pi}G_\sigma^<(E) = i\int\frac{dE}{2\pi}\frac{\Gamma_\sigma^L f_L(E) + \Gamma_\sigma^R f_R(E)}{\Gamma_\sigma^L+\Gamma_\sigma^R}[G_\sigma^r(E) - G_\sigma^a(E)]. \tag{7}$$

In the following the parameters Γ_σ^β will be used to parameterize the strength of the coupling between the dot and leads. It is convenient to introduce the spin polarization factors p_β defined as $p_\beta = (\Gamma_+^\beta - \Gamma_-^\beta)/(\Gamma_+^\beta + \Gamma_-^\beta)$, where Γ_+^β and Γ_-^β are the coupling parameters for spin-majority and spin-minority electrons in the lead β, respectively. Accordingly, one may write $\Gamma_+^\beta = (1+p_\beta)\Gamma^\beta$ and $\Gamma_-^\beta = (1-p_\beta)\Gamma^\beta$, with $\Gamma^\beta = (\Gamma_+^\beta + \Gamma_-^\beta)/2$.

The retarded (advanced) Green function $G_\sigma^{r(a)}$ of the dot can be calculated only approximately, for instance by the equation of motion method. In the approximations introduced by Meir *et al* [5] one finds

$$G_\sigma^r(E) = \frac{E - \epsilon_\sigma - U(1-n_{-\sigma})}{[E-\epsilon_\sigma - \Sigma_\sigma^r(E)](E-\epsilon_\sigma-U) - Un_{-\sigma}\Sigma_\sigma^r(E)}, \tag{8}$$

where Σ_σ^r is the corresponding self energy,

$$\Sigma_\sigma^r(E) = \Sigma_{0\sigma}^r(E) + U\frac{(E-\epsilon_\sigma)n_{-\sigma}\Sigma_{03\sigma}^r(E) - L_{0\sigma}\Sigma_{01\sigma}^r(E)}{L_{0\sigma}(E)[L_{0\sigma}(E) - \Sigma_{03\sigma}^r(E)]}, \tag{9}$$

with $L_{0\sigma} = E - \epsilon_\sigma - U(1-n_{-\sigma})$, and $\Sigma_{01\sigma}^r(E)$ and $\Sigma_{03\sigma}^r(E)$ defined as

$$\Sigma_{01\sigma}^r(E) = n_{-\sigma}\Sigma_{0\sigma}^r(E) + \Sigma_{1\sigma}^r(E), \tag{10}$$

$$\Sigma_{03\sigma}^r(E) = \Sigma_{0\sigma}^r(E) + \Sigma_{3\sigma}^r(E). \tag{11}$$

The self-energies $\Sigma_{0\sigma}^r(E)$, $\Sigma_{1\sigma}^r(E)$, and $\Sigma_{3\sigma}^r(E)$ are defined as

$$\Sigma_{0\sigma}^r(E) = \sum_{\beta=L,R}\Sigma_{0\sigma}^{\beta r}(E) = \sum_{\beta=L,R}\sum_k |V_{k\beta\sigma}|^2\frac{1}{E-\varepsilon_{k\beta\sigma}+i0^+}$$
$$= \sum_{\beta=LR}\int\frac{d\varepsilon}{2\pi}\frac{\Gamma_\sigma^\beta}{E-\varepsilon} - i\frac{\Gamma_\sigma^\beta}{2} \tag{12}$$

and

$$\Sigma_{i\sigma}^r(E) = \sum_{\beta=LR}\int\frac{d\varepsilon}{2\pi}A_i\Gamma_{-\sigma}^\beta\left[\frac{1}{\varepsilon+E-\epsilon_{-\sigma}-\epsilon_\sigma-U-i\hbar/\tau_{-\sigma}}\right.$$
$$\left. - \frac{1}{\varepsilon-E-\epsilon_{-\sigma}+\epsilon_\sigma-i\hbar/\tau_{-\sigma}}\right], \tag{13}$$

(for $i = 1, 3$), where $A_1 = f(\varepsilon)$, $A_3 = 1$, and $\tau_{-\sigma}$ is the relaxation time of the intermediate states [5]. This relaxation time is spin dependent and in the low-temperature limit is given by the formula [5]

$$\frac{1}{\tau_\sigma} = \frac{1}{2\pi\hbar} \sum_{\beta,\beta'} \sum_{\sigma'} \Gamma_\sigma^\beta \Gamma_{\sigma'}^{\beta'} \Theta(\mu_{\beta'} - \mu_\beta + \epsilon_\sigma - \epsilon_{\sigma'}) \frac{\mu_{\beta'} - \mu_\beta + \epsilon_\sigma - \epsilon_{\sigma'}}{(\mu_\beta - \epsilon_\sigma)(\mu_{\beta'} - \epsilon_{\sigma'})}, \tag{14}$$

where $\Theta(x) = 0$ for $x < 0$ and $\Theta(x) = 1$ otherwise.

In the limit of infinite U the Green function (8) reduces to the well known form,

$$G_\sigma^r(E) = \frac{1 - n_{-\sigma}}{E - \epsilon_\sigma - \Sigma_{0\sigma}^r(E) - \Sigma_{1\sigma}^r(E)}, \tag{15}$$

where $\Sigma_{0\sigma}^r(E)$ is given by equation (12) and $\Sigma_{1\sigma}^r(E)$ by

$$\Sigma_{1\sigma}^r(E) = \sum_{\beta=\mathrm{L,R}} \Sigma_{1\sigma}^{\beta r}(E) \equiv \sum_{\beta=\mathrm{L,R}} \int \frac{\mathrm{d}\varepsilon}{2\pi} \frac{f_\beta(\varepsilon)\Gamma_{-\sigma}^\beta}{-\varepsilon + E + \epsilon_{-\sigma} - \epsilon_\sigma + \mathrm{i}\hbar/\tau_{-\sigma}}, \tag{16}$$

with τ_σ defined by equation (14).

The above-derived Green functions are sufficient to describe qualitatively basic features of the Kondo phenomenon in QDs attached to nonmagnetic leads [5]. However, they are not sufficient to describe the Kondo phenomenon correctly when the quantum dot is attached to ferromagnetic leads. The key feature of the system which is not properly described is the splitting of the dot level due to spin-dependent tunnelling processes [19]. In this paper we take into account the level splitting by replacing the bare energy levels with the renormalized ones in a self-consistent way. The main contribution to the level renormalization comes from the self-energy $\Sigma_{1\sigma}^r(E)$ and is given by $\Delta\epsilon_\sigma = \Sigma_{1\sigma}^r(E = \epsilon_\sigma)$. This renormalization allows us to introduce the effective exchange field $g\mu_\mathrm{B}B_\mathrm{ex} = \Delta\epsilon_\uparrow - \Delta\epsilon_\downarrow$. Thus, on taking into account equation (13), the exchange field B_ex can be expressed by the formula

$$B_\mathrm{ex} = \frac{1}{g\mu_\mathrm{B}} \sum_{\beta=R,L} \mathrm{Re} \int \frac{\mathrm{d}\varepsilon}{2\pi} f_\beta(\varepsilon) \left[\Gamma_\uparrow^\beta \left(\frac{1}{\varepsilon - \epsilon_\uparrow - \mathrm{i}\hbar/\tau_\uparrow} - \frac{1}{\varepsilon - \epsilon_\uparrow - U - \mathrm{i}\hbar/\tau_\uparrow} \right) \right.$$
$$\left. - \Gamma_\downarrow^\beta \left(\frac{1}{\varepsilon - \epsilon_\downarrow - \mathrm{i}\hbar/\tau_\downarrow} - \frac{1}{\varepsilon - \epsilon_\downarrow - U - \mathrm{i}\hbar/\tau_\downarrow} \right) \right]. \tag{17}$$

When the bare dot level and spin relaxation time are independent of the spin orientation, $\epsilon_\uparrow = \epsilon_\downarrow = \epsilon$ and $\tau_\uparrow = \tau_\downarrow = \tau$, formula (17) acquires the form [35]

$$B_\mathrm{ex} = \frac{1}{g\mu_\mathrm{B}} \sum_{\beta=R,L} \mathrm{Re} \int \frac{\mathrm{d}\varepsilon}{2\pi} f_\beta(\varepsilon) \left(\Gamma_\uparrow^\beta - \Gamma_\downarrow^\beta \right) \left(\frac{1}{\varepsilon - \epsilon - \mathrm{i}\hbar/\tau} - \frac{1}{\varepsilon - \epsilon - U - \mathrm{i}\hbar/\tau} \right). \tag{18}$$

The above description is self-consistent and takes into account the main features following from ferromagnetism of the electrodes. These features are described here effectively by the exchange field B_ex. We also want to emphasize that the results obtained within such an approach are in agreement with the relevant experimental data [25]. Moreover, the results are also consistent with those obtained recently by a real time diagrammatic technique [36].

4. Numerical results

Now, we apply the above described formalism to the Kondo problem in a QD coupled to ferromagnetic leads. In the numerical calculations described below the energy is measured in the units of D, where $D = \bar{D}/50$ and $\bar{D}$ is the electron band width. For simplicity, the electron band in the leads is assumed to be independent of the spin orientation and extends from $-25D$

below the Fermi level (bottom band edge) up to $25D$ above the Fermi level (top band edge). The energy integrals will be cut off at $E = \pm 25D$, i.e., will be limited to the electron band. Thus, the influence of ferromagnetic electrodes is included only *via* the spin asymmetry of the coupling parameters $\Gamma_\sigma^{\mathrm{L}}$ and $\Gamma_\sigma^{\mathrm{R}}$. Apart from this, in all numerical calculations we assumed $kT/D = 0.001$ and $\epsilon_{0\uparrow}/D = \epsilon_{0\downarrow}/D = \epsilon_0/D = -0.35$.

For positive (negative) bias we assume the electrostatic potential of the left (right) electrode to be equal to zero. In other words, the electrochemical potential of the drain electrode is assumed to be zero while of the source electrode is shifted up by $|eV|$. In the following the bias is described by the corresponding electrostatic energy eV. Note that positive eV corresponds to negative bias due to negative electron charge ($e < 0$).

4.1. QD coupled to two similar ferromagnetic leads

Consider first the situation when both electrodes are made of the same ferromagnetic metal, and the coupling of the dot to both leads is symmetrical (in the parallel configuration). For numerical calculations we assumed $\Gamma_+^{\mathrm{L}}/D = \Gamma_+^{\mathrm{R}}/D = 0.12$ for spin-majority electrons and $\Gamma_-^{\mathrm{L}}/D = \Gamma_-^{\mathrm{R}}/D = 0.08$ for spin-minority ones, which corresponds to the spin polarization factor $p_{\mathrm{L}} = p_{\mathrm{R}} = p = 0.2$, and $\Gamma^{\mathrm{L}}/D = \Gamma^{\mathrm{R}}/D = 0.1$.

It was shown in [19] that ferromagnetism of the electrodes leads to spin splitting of the Kondo peak in the density of states (DOS) in the parallel configuration, whereas no splitting occurs for the antiparallel orientation. Such a behaviour of the DOS has a significant influence on the transport properties. First of all, the Kondo peak in the DOS leads to a zero-bias anomaly in the differential conductance $G_{\mathrm{diff}} = \partial I/\partial V$. This anomaly is particularly interesting in the parallel configuration, where the spin splitting of the Kondo peak in the DOS leads to splitting of the differential conductance, as shown in figure 1(a) for four different values of the electrode spin polarization factor p and for large U. For $p = 0$ there is only a single peak centred at zero bias. When the polarization factor becomes nonzero, the peak becomes split into two components located symmetrically on both sides of the original peak, with the corresponding intensities significantly suppressed. The splitting of the Kondo anomaly increases with increasing p. Moreover, the height of the two components of the Kondo anomaly decreases with increasing p. On the other hand, in the antiparallel configuration there is no splitting of the Kondo peak in the DOS and consequently also no splitting of the Kondo anomaly in the differential conductance (see figure 1(b)). For all polarization values, the anomaly is similar to that in the case of QDs coupled to nonmagnetic leads. However, the intensity of the Kondo anomaly decreases with increasing polarization. The difference between the conductance in the antiparallel and parallel configurations gives rise to the tunnel magnetoresistance (TMR) effect which may be described quantitatively by the ratio $(I^{\mathrm{P}} - I^{\mathrm{AP}})/I^{\mathrm{AP}}$, where I^{P} and I^{AP} denote the current flowing through the system in the parallel and antiparallel configurations at the same bias, respectively. The associated TMR effect is displayed in figure 1(c). One finds negative values of the TMR ratio, which is a consequence of the spin-splitting of the Kondo peak in the parallel configuration and the absence of such a splitting for antiparallel alignment. It is worth noting that in the absence of the Kondo anomaly the TMR effect would be positive.

The Kondo anomaly in transport characteristics shown in figure 1 was calculated for the limit of large U. In figure 2 we show similar characteristics as in figure 1, but for different values of the correlation parameter U and a constant value of the polarization factor p. The splitting of the Kondo anomaly in the parallel configuration and the intensity of the peaks (figure 2(a)) decrease with decreasing U. In the antiparallel configuration there is no splitting of the Kondo anomaly, but the intensity of the Kondo peak decreases with decreasing U. The associated TMR effect is shown in figure 2(c). The effect is negative in a certain bias

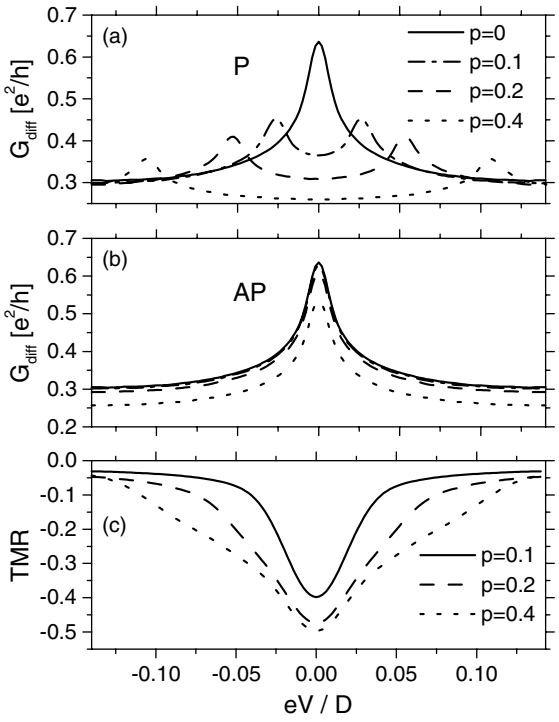

Figure 1. Bias dependence of the differential conductance in the parallel (a) and antiparallel (b) configurations, and the corresponding TMR (c) for the indicated four values of the lead polarization $p_{\mathrm{L}} = p_{\mathrm{R}} = p$ ($p = 0$ corresponds to nonmagnetic leads so the corresponding TMR vanishes and is not shown in part (c)). The parameters assumed for numerical calculations are: $kT/D = 0.001$, $\Gamma^{\mathrm{L}}/D = \Gamma^{\mathrm{R}}/D = 0.1$, $\epsilon_{0\uparrow}/D = \epsilon_{0\downarrow}/D = \epsilon_0/D = -0.35$, $U/D = 500$, and $(e^2/C_{\mathrm{L}})/D = (e^2/C_{\mathrm{R}})/D = 0.33$.

range around the zero-bias limit, but the absolute magnitude of the effect becomes smaller for smaller values of U. For large bias there is a transition from negative to positive TMR with decreasing U.

4.2. QD coupled to one ferromagnetic lead and one half-metallic lead

Assume now that one of the electrodes (say the left one) is made of a 3d ferromagnetic metal, the second (right) one is half-metallic, and the total coupling to the latter electrode is much smaller than to the former one. This is reflected in the spin asymmetry of the bare coupling constants, for which we assume $\Gamma^{\mathrm{L}}_{+}/D = 0.28$ and $\Gamma^{\mathrm{L}}_{-}/D = 0.12$ for the left electrode, and $\Gamma^{\mathrm{R}}_{+}/D = 0.04$ and $\Gamma^{\mathrm{R}}_{-}/D = 0.0002$ for the right one. These parameters correspond to $p_{\mathrm{L}} = 0.4$, $p_{\mathrm{R}} = 0.99$, $\Gamma^{\mathrm{L}}/D = 0.2$, and $\Gamma^{\mathrm{R}}/D \approx 0.02$. Thus, the spin asymmetry of the coupling to the right electrode is much larger than to the left one. In figure 3 we show the DOS in the parallel (left column) and antiparallel (right column) magnetic configurations, calculated for vanishing as well as for positive and negative bias voltages. Consider now the main features of the spectra in more details, and let us begin with the parallel configuration (left column in figure 3).

At $V = 0$ the Kondo peak in the DOS is spin-split, and the intensity of the spin-down peak is relatively large, whereas that of the spin-up peak is much smaller. The asymmetry

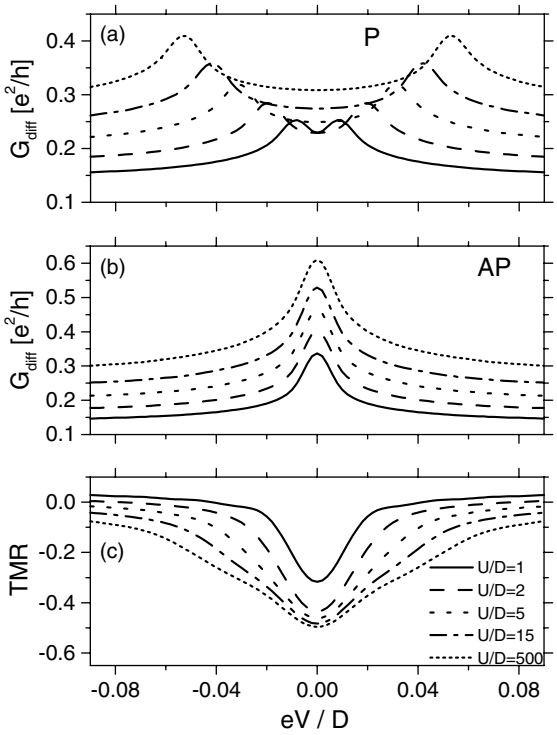

Figure 2. Bias dependence of differential conductance in the parallel (a) and antiparallel (b) configurations, and the corresponding TMR (c) calculated for indicated values of the correlation parameter U and for $p = 0.2$. The other parameters are as in figure 1.

in peak intensities is a consequence of the spin asymmetry in the coupling of the dot to metallic electrodes—this coupling is larger for a spin-up electron, which determines the height of the Kondo peak for spin-down electrons. When a bias voltage is applied, each of the two Kondo peaks generally becomes additionally split into two components. One of them (the one associated with the coupling to the source electrode) moves up in energy, whereas the position of the second one (the one associated with the drain electrode) remains unchanged. This is because we assumed that the electrochemical potential of the source electrode shifts up by $|eV|$, while that of the drain electrode is independent of the voltage. For $eV > 0$ (negative bias), the splitting of the large-intensity (spin-down) peak is clearly visible, although one component of the split peak is relatively small. This is just the component associated with the coupling of the dot to the right electrode in the spin-up channel. Since this coupling is relatively small, the corresponding intensity is also small. The second component, in turn, is much larger because it is associated with the coupling to the left electrode in the spin-up channel, which is the dominant coupling in the system considered. Splitting of the low-intensity (spin-up) peak is not resolved. The intensity of the component associated with the coupling to the right electrode in the spin-down channel practically vanishes because this coupling is negligible in the case considered. For $eV < 0$ (positive bias), the situation is changed. Now the electrochemical potential of the left electrode is independent of the bias. Consequently, the intensity of the components whose position is independent of energy is significantly larger than the intensity of the other components (the ones associated with the right electrode). As before, the component associated with the coupling to the right electrode in the spin-down channel is not resolved.

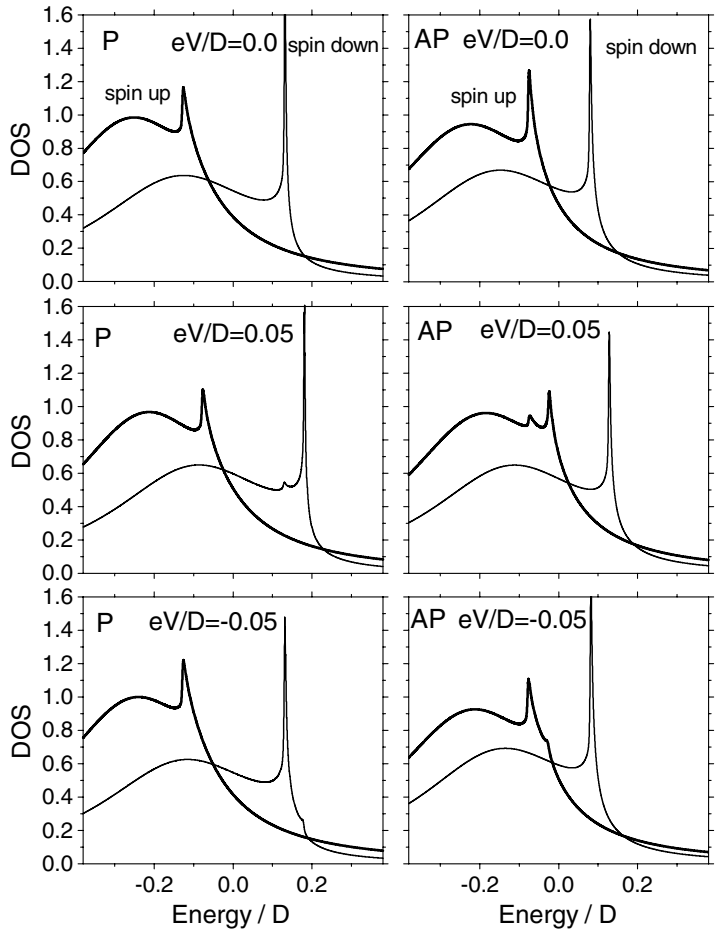

Figure 3. DOS for spin-up (thick lines) and spin-down (thin lines) electron states on the dot in the parallel (left column) and antiparallel (right column) magnetic configurations, calculated for three indicated voltages and for $\Gamma_+^{\mathrm{L}}/D = 0.28$, $\Gamma_-^{\mathrm{L}}/D = 0.12$, $\Gamma_+^{\mathrm{R}}/D = 0.04$, $\Gamma_-^{\mathrm{R}}/D = 0.0002$, $U/D = 500$, $(e^2/C_{\mathrm{L}})/D = (e^2/C_{\mathrm{R}})/D = 10$. The other parameters are as in figure 1.

Consider now the antiparallel configuration (right column in figure 3), when the magnetic moment of the right electrode is reversed. There is a nonzero spin splitting of the Kondo peak at equilibrium, contrary to the case of symmetric coupling to the magnetic electrodes, where the spin splitting in the antiparallel configuration vanishes [19]. Apart from this, the situation is qualitatively similar to that for the parallel configuration. The main difference is that now the bias-induced splitting of the large-intensity peak is not resolved, whereas the splitting of the low-intensity peak is resolved.

As in the case of symmetrical coupling described above, the Kondo peaks in the DOS give rise to anomalous behaviour of the corresponding transport characteristics. Due to the splitting of the equilibrium Kondo peak, the anomaly in the DOS does not contribute to transport in the small-bias regime. The Kondo peaks enter the 'tunnelling window' at a certain bias, which leads to an enhanced conductance. Such an enhancement is clearly visible in the current–voltage characteristics shown in figure 4 for both parallel (a) and antiparallel (b) configurations (solid lines), where for negative values of eV the enhancement is quite significant, but it is

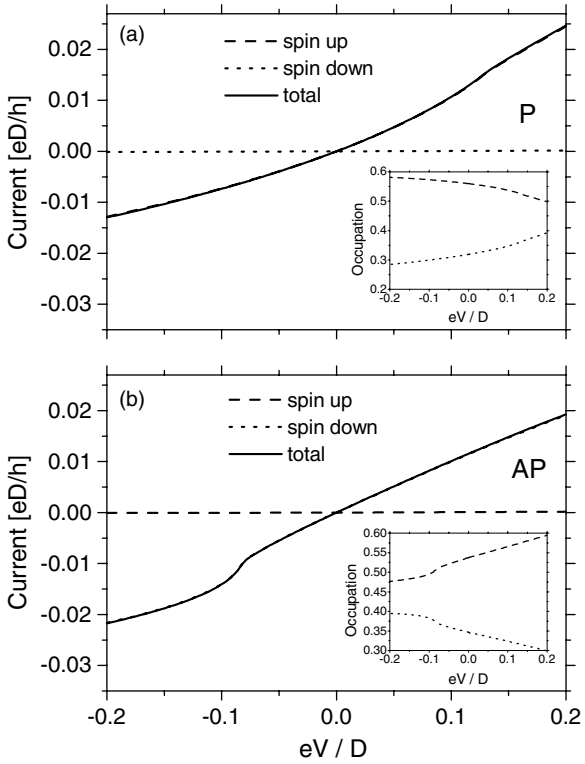

Figure 4. Current–voltage characteristics in the parallel (a) and antiparallel (b) configurations, calculated for the parameters as in figure 3. Current in the spin-down (spin-up) channel in the parallel (antiparallel) configuration almost vanishes so the total current flows in the spin-up (spin-down) channel (the curves presenting the total and spin-up (spin-down)) currents are not resolved. The insets show the corresponding occupation numbers. The parameters as in figure 3.

less pronounced for $eV > 0$. This asymmetry is due to the difference in intensities of the corresponding Kondo peaks that enter the 'tunnelling window'.

The differential conductance in the Kondo regime is shown in figure 5 for parallel (a) and antiparallel (b) magnetic configurations. In the parallel configuration the Kondo anomaly occurs in the spin-up channel and for $eV > 0$ only. This may be easily understood by considering the relevant DOS (see figure 3, left column). For $eV > 0$ only the Kondo peak in the spin-up DOS can enter the tunnelling window created by the bias. For $eV < 0$, on the other hand, the Kondo peak in the spin-down DOS can enter the tunnelling window. However, the spin-down channel is almost nonconducting, so the corresponding peak in the differential conductance is suppressed. In the antiparallel configuration the Kondo peak in differential conductance occurs for $eV < 0$ only. This can be accounted for by taking into account the behaviour of the Kondo peaks in the DOS shown in figure 3 (right column), and the fact that now the spin-up channel is nonconducting. For $eV > 0$ only the Kondo peak in the spin-up DOS can enter the tunnelling window, whereas for $eV < 0$ this is the Kondo peak in the spin-down DOS (of large intensity).

The corresponding TMR is shown in figure 5(c). It is interesting to note that the TMR is highly asymmetrical with respect to the bias reversal. It becomes positive for eV exceeding a certain positive value, and negative below this voltage. This is a consequence of the fact that

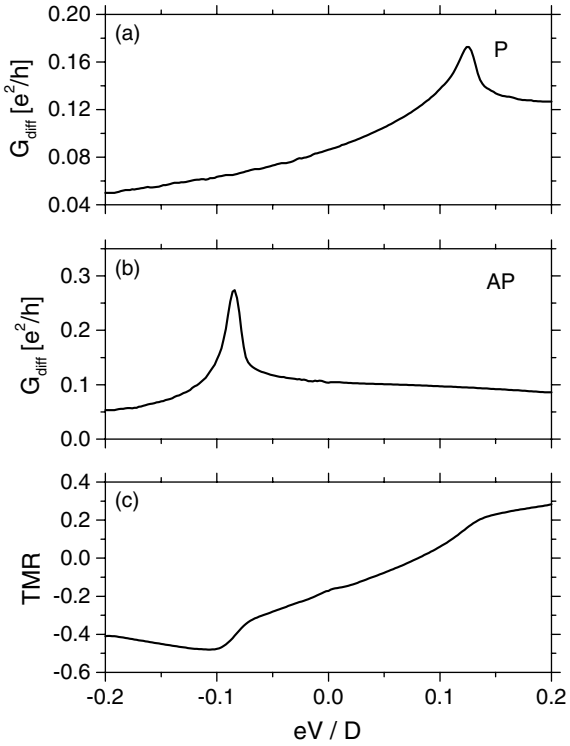

Figure 5. Bias dependence of the differential conductance in the parallel (a) and antiparallel (b) configurations and the corresponding TMR (c), calculated for the same parameters as in figure 3.

for positive eV the Kondo peak in the differential conductance is clearly visible in the parallel configuration (see figure 5(a)), whereas for $eV < 0$ the Kondo peak occurs in the antiparallel configuration (see figure 5(b)). Such a behaviour of the conductance and also the TMR may be interesting from the point of view of applications in mesoscopic diodes.

4.3. QD coupled to one ferromagnetic lead and one nonmagnetic lead

A specific example of asymmetric systems is the case where one electrode is ferromagnetic (typical ferromagnetic 3d metal) whereas the second one is nonmagnetic. For numerical calculations we assumed $\Gamma_+^{\mathrm{L}}/D = 0.12$, $\Gamma_-^{\mathrm{L}}/D = 0.08$ for the left (magnetic) electrode, and $\Gamma_+^{\mathrm{R}}/D = \Gamma_-^{\mathrm{R}}/D = 0.1$ for the right (nonmagnetic) one, which corresponds to $p_{\mathrm{L}} = 0.2$, $p_{\mathrm{R}} = 0$, and $\Gamma^{\mathrm{L}}/D = \Gamma^{\mathrm{R}}/D = 0.1$. As in the other asymmetrical situations studied in this paper, the equilibrium Kondo peak in the DOS becomes spin-split. When a bias voltage is applied, each component becomes additionally split, as shown in figure 6. Variation of the spectra with bias voltage can be accounted for in a similar way as in the case of the dot coupled asymmetrically to two ferromagnetic electrodes. The only difference is that now all components of the peaks are clearly resolved. This is because all coupling constants are now of comparable magnitude.

The corresponding differential conductance is shown in figure 7. Due to the spin splitting of the Kondo peak in the DOS, the Kondo anomaly in the conductance becomes split as well, as

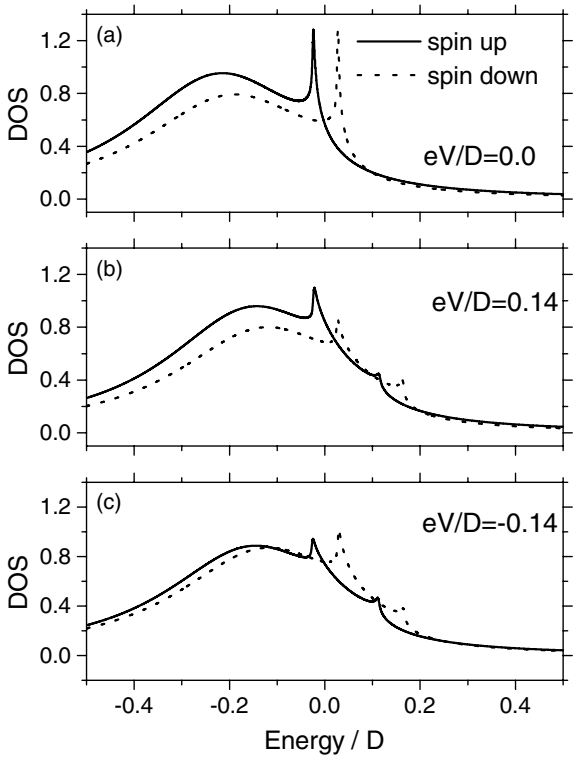

Figure 6. DOS for spin-up (solid lines) and spin-down (dotted lines) electron states of the dot, calculated for three different voltages, and for $\Gamma_+^{\mathrm{L}}/D = 0.12$, $\Gamma_-^{\mathrm{L}}/D = 0.08$, $\Gamma_+^{\mathrm{R}}/D = \Gamma_-^{\mathrm{R}}/D = 0.1$, $U/D = 500$, and $(e^2/C_{\mathrm{L}})/D = (e^2/C_{\mathrm{R}})/D = 0.33$. The other parameters are as in figure 1.

is clearly seen in figure 7. However, the splitting is asymmetric with respect to the bias reversal. Thus, there is no need to have two ferromagnetic electrodes to observe splitting of the Kondo anomaly, but it is sufficient when only one lead is ferromagnetic.

5. Summary and conclusions

In this paper we considered the Kondo problem in quantum dots coupled symmetrically and asymmetrically to ferromagnetic leads. As a specific example of asymmetrical systems, we considered the case when one electrode is ferromagnetic, whereas the second one is nonmagnetic.

We showed that ferromagnetism of the leads gives rise to a splitting of the equilibrium Kondo peak in the DOS for all asymmetrical situations. This generally takes place for both magnetic configurations when the two electrodes are different. The splitting in both configurations also occurs when both magnetic electrodes are of the same material, but the corresponding coupling strengths to the dot are different. Indeed, such a splitting in parallel and also antiparallel configurations was recently observed experimentally [25]. When similar electrodes are symmetrically coupled to the dot, the splitting occurs only in the parallel configuration. An interesting conclusion from the experimental point of view is that the splitting also occurs in the case when one electrode is nonmagnetic.

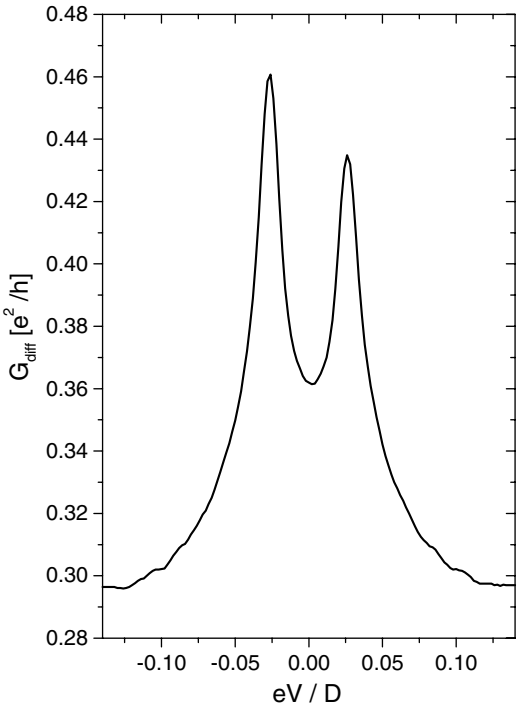

Figure 7. Bias dependence of the differential conductance, calculated for the parameters as in figure 6.

The spin-splitting of DOS can lead to characteristic splitting of the zero-bias anomaly in electrical conductance. This in turn can lead to a negative (inverse) TMR effect. In highly asymmetrical systems the TMR can change sign when the bias voltage is reversed.

Acknowledgments

The work was supported by the State Committee for Scientific Research through the Research Project PBZ/KBN/044/P03/2001 and 4 T11F 014 24.

References

[1] Glazman L I and Raikh M E 1988 *JETP Lett.* **47** 452
Ng T K and Lee P A 1988 *Phys. Rev. Lett.* **61** 1768
[2] Cronenwett S M, Oosterkamp T H and Kouvenhoven L P 1998 *Science* **281** 540
Sasaki S, De Franceschi S, Elzerman J M, van der Wiel W G, Eto M, Tarucha S and Kouvenhoven L P 2000 *Nature* **405** 764
[3] Gores J, Goldhaber-Gordon D, Heemeyer S, Kastner M A, Shtrikman H, Mahalu D and Meirav U 2000 *Phys. Rev.* B **62** 2188
[4] Hershfield S, Davies J H and Wilkins J W 1991 *Phys. Rev. Lett.* **67** 3720
[5] Meir Y, Wingreen N S and Lee P A 1993 *Phys. Rev. Lett.* **70** 2601
[6] Levy-Yeyati A, Martin-Rodero A and Flores F 1993 *Phys. Rev. Lett.* **71** 2991
Levy-Yeyati A, Flores F and Martin-Rodero A 1999 *Phys. Rev. Lett.* **83** 600
[7] Wingreen N S and Meir Y 1994 *Phys. Rev.* B **49** 11040
[8] Kang K and Min B I 1995 *Phys. Rev.* B **52** 10689

[9] Palacios J J, Liu L and Yoshioka D 1997 *Phys. Rev.* B **55** 15735
[10] Schöller H and König J 2000 *Phys. Rev. Lett.* **84** 3686
[11] Krawiec M and Wysokiński K I 2002 *Phys. Rev.* B **66** 165408
[12] Costi T A 2000 *Phys. Rev. Lett.* **85** 1504
Costi T A 2001 *Phys. Rev.* B **64** 241310
[13] Moore J E and Wen X-G 2000 *Phys. Rev. Lett.* **85** 1722
[14] Kaminski A, Nazarov Yu V and Glazman L I 2000 *Phys. Rev.* B **62** 8154
[15] Lee Y W and Lee Y L 2001 *Preprint* cond-mat/0105009
[16] Czycholl G 1985 *Phys. Rev.* B **31** 2867
[17] Haug H and Jauho A-P 1996 *Quantum Kinetics in Transport and Optics of Semiconductors* (Berlin: Springer)
[18] Sergueev N, Sun Q F, Guo H, Wang B G and Wang J 2002 *Phys. Rev.* B **65** 165303
[19] Martinek J, Utsumi Y, Imamura H, Barnaś J, Maekawa S, König J and Schön G 2003 *Phys. Rev. Lett.* **91** 127203
[20] Lü R and Liu Z R 2002 *Preprint* cond-mat/0210350
[21] Bułka B R and Lipiński S 2003 *Phys. Rev.* B **67** 024404
[22] Lopez R and Sanchez D 2003 *Phys. Rev. Lett.* **90** 116602
[23] Choi M S, Sanchez D and Lopez R 2004 *Phys. Rev. Lett.* **92** 056601
[24] Martinek J, Sindel M, Borda L, Barnaś J, König J, Schön G and von Delft J 2003 *Phys. Rev. Lett.* **91** 247202
[25] Pasupathy A N, Bialczak L C, Martinek J, Grose J E, Donev L A K, McEuen P L and Ralph D C 2004 *Science* **306** 86
[26] Rudzinski W and Barnaś J 2001 *Phys. Rev.* B **69** 085318
[27] Świrkowicz R, Barnaś J, Wilczyński M, Rudzinski W and Dugaev V D 2004 *J. Magn. Magn. Mater.* **272–276** 1959
[28] Wang B, Wang J and Guo H 1999 *J. Appl. Phys.* **86** 5094
[29] Świrkowicz R, Barnaś J and Wilczyński M 2002 *J. Phys.: Condens. Matter* **14** 2011
[30] Jauho A P, Wingreen N S and Meir Y 1994 *Phys. Rev.* B **50** 5528
[31] Świrkowicz R, Barnaś J and Wilczyński M 2003 *Phys. Rev.* B **68** 195318
[32] Niu C, Lin D L and Lin T H 1999 *J. Phys.: Condens. Matter* **11** 1511
[33] Kang K 1998 *Phys. Rev.* B **57** 11891
[34] Sun Q-F and Guo H 2002 *Phys. Rev.* B **66** 155308
[35] Braun M, König J and Martinek J 2004 *Phys. Rev.* B **70** 195345
[36] Utsumi Y, Martinek J, Schön G, Imamura H and Maekawa S 2005 *Phys. Rev.* B **71** 245116